*COST B21 „Physiological modelling of MR image formation"*

# Approaches to MRI simulation

Paweł Majewski, Andrzej Materka

Cyprus, 1 October 2004

## *Why simulation?*

- complement to real, costly MRI measurements
- understanding of the method (varying parameters, sequences,…)
- educational tool in medical and technical environments
- study of artefacts (e.g. their comparison for different sequences)
- development and optimization of sequences
- comparisons of registration and segmentation algorithms

## *Classification of methods (1)*

- based on partial or approximate solutions of the Bloch equation with respect to the MR image contrast behaviour
- no account of hardware errors and some physical effects
- differ in the extent of applicability, accuracy, and computation effort
- well-suited mainly for medical and technical education


- Torheim G, Rinck PA. Jones RA, Kvaerness J, **1994, A simulator for teaching MR image contrast behaviour MAGMA** 2:515-522
- Rundle D, Kishore S, Seshadri S, Wehrli F, **1990, Magnetic Resonancce Imaging Simulator: A teaching tool for radiology, Journal of Digital Imaging** 3(4):226-229

## *Classification of methods (2)*

- based on the k-space formalism
- permits only linear effects to be taken into account
- not able to cover nonlinear gradients or objects distortions due to inhomogeneous main magnetic field
- very fast
- lacks generality

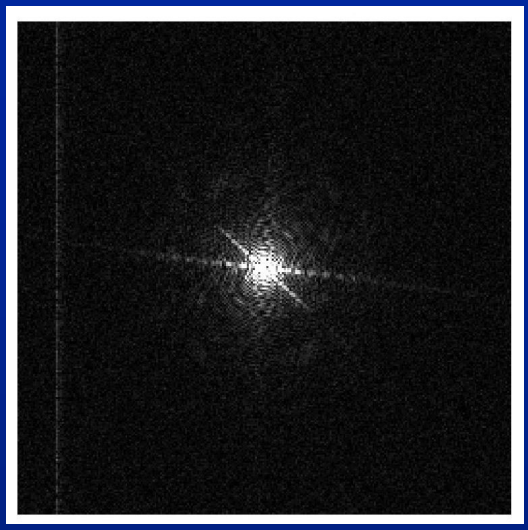

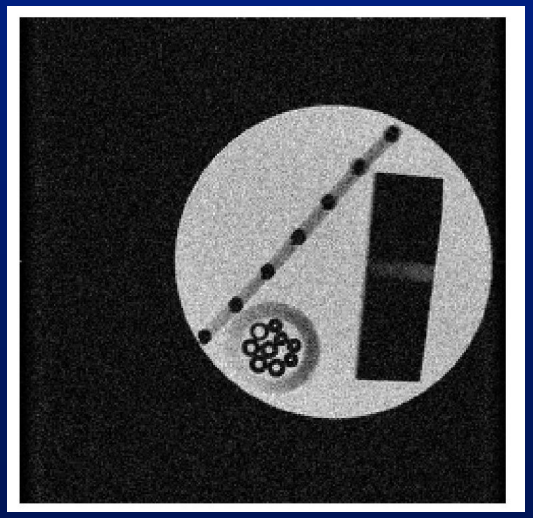

• Petterson J S, Christoffersson J O, Golman K, **1993, MRI simulation using the k-space formalism, Magnetic Resonance Imaging** 11:557-568

## *Classification of methods (3)*

- solution of Bloch's equation employing matrix operators
- most general modelling of the imaging process
- decomposing the object into spin attributed with a magnetization vector and local properties like relaxation
- superposition of all spins yields the MR signal
- often results in huge demands on computer memory and speed
- early simulators lacked generality, e.g. because of a limited set of main field inhomogeneity distributions


- Bittoun J, Taquin J, Sauzade M, **1984, A Computer Algorithm for the Simulation of any Nuclear Magnetic Resonance Imaging Method, Magn. Res. Imag.** 2:113-120
- Summers R M, Axel L, Israel S, **1986, A Computer Simulation of Nuclear Magnetic Resonance Imaging, Magnetic Resonance in Medicine** 3:363-376

## *Recent projects*

## *P Majewski, A Materka: Approaches to MRI Simulation*

ELSEVIER

Magnetic Resonance Imaging 22 (2004) 315–328

MAGNETIC RESONANCE IMAGING

MRI simulator with object-specific field map calculations[1]

Duane A. Yoder[a], Yansong Zhao[b], Cynthia B. Paschal[b,c,d], J. Michael Fitzpatrick[b,d,e,*]

***Includes***

- object-specific inhomogeneities and static field errors
- chemical-shift
- intravoxel dephasing applied throughout the acquisition protocol

***Two parts***

- static field perturbation
- signal and image generation

Ignores RF inhomogeneity, eddy currents and gradient nonlinearity.

## *Inputs*

- Object definition
- Object-specific inhomogeneities
- Applied static field errors
- Chemical shift values
- Description of the acquisition protocols

MR simulator

## *Output*

- time sequence of complex numbers organized into k-space;
- image produced by means of a Fourier transform

# Theory (1)

## The Bloch equation

$$\frac{d\vec{M}}{dt} = \gamma \cdot (\vec{M} \times \vec{B}) - \begin{pmatrix} M_x/T_2 \\ M_y/T_2 \\ (M_z - M_0)/T_1 \end{pmatrix}$$

$\vec{M} = (M_x, M_y, M_z)^T$ - magnetization vector

$M_0$ – magnetization at thermal equilibrium

$T_1, T_2$ – spin-lattice and spin-spin ralaxations

$\vec{B}$ - flux of the magnetic field

## $\vec{B}$ - flux of the magnetic field

$$\vec{B} = \vec{B}_0 + \Delta\vec{B} + (\vec{G}(t) \cdot \vec{r})\vec{e}_z + \vec{B}_1(t)$$

$\vec{B}_0 = B_0 \cdot \vec{e}_z$ - main magnetic field

$\Delta\vec{B}$ - inhomogeneity

$\vec{G}(t)$ - applied gradients

$\vec{r} = (x, y, z)^T$ - position in space

$\vec{B}_1(t)$ - magnetic flux of RF pulses

$\vec{e}_z$ - unit vector in the z direction

## Theory (2)

### Solution of the Bloch equation

$$\vec{M}(\vec{r}, t+\Delta t) = \boldsymbol{R}_{grad} \cdot \boldsymbol{R}_{inh} \cdot \boldsymbol{R}_{relax} \cdot \boldsymbol{R}_{RF} \cdot \vec{M}(\vec{r}, t) + M_0(\vec{r})\left(1 - e^{-\frac{t}{T_1(\vec{r})}}\right)\vec{e}_z.$$

$R_{grad}$ – influence of the applied gradients
$R_{inh}$ – main field inhomogeneity
$R_{relax}$ – effect of relaxation
$R_{RF}$ – rotating properties of the RF pulse

## *Implementation*

- The core: Matlab 6.1
- Computation of the field for 181 x 217 x 181 1 $mm^3$ voxels phantom, performed on 1,5 GHz Pentium 4 with 256 MB memory takes 19,5 hours

## Validation (experimental data)

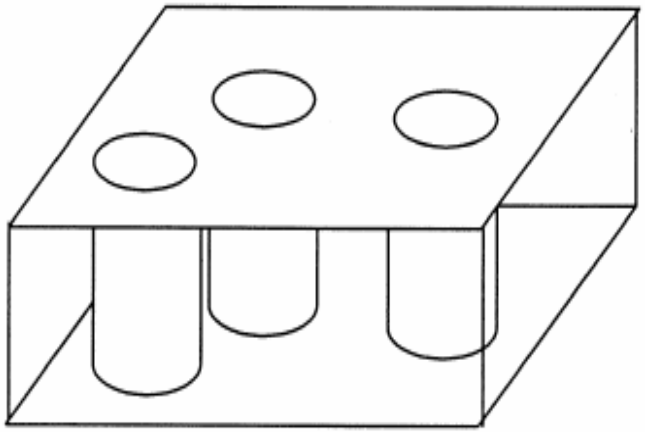

Fig. 4. A diagram of the "sinus" phantom constructed to model air/tissue interfaces. Each cylinder was filled with air with the remainder of the phantom containing distilled water. The width, depth, and height of the phantom are 12 cm, 6.6 cm, and 5.2 cm, respectively.

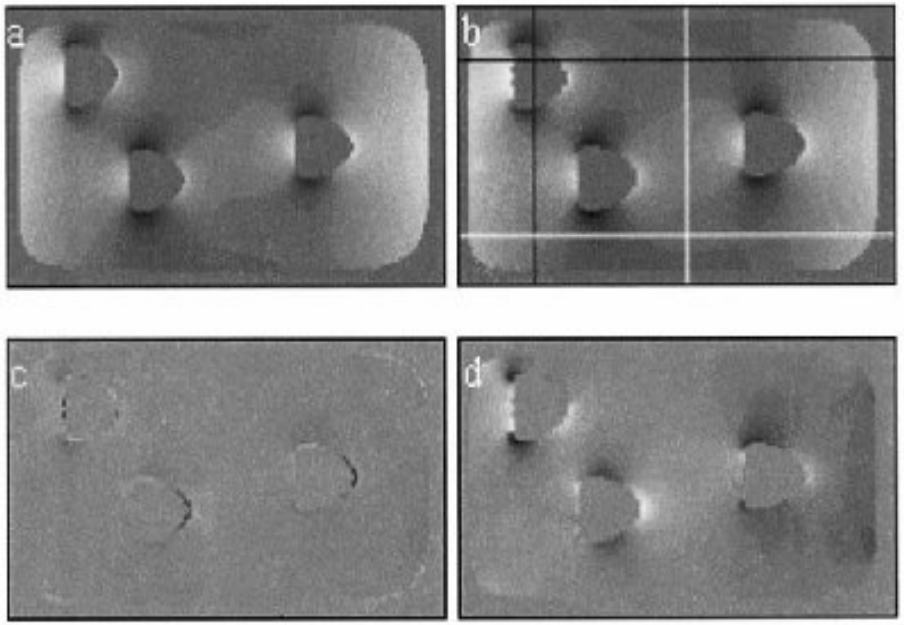


Fig. 7. The perturbed field (a) measured by experiment and (b) calculated by SVC. The range of (a) and (b) is from –2.95 ppm (black) to 5.3 ppm (white). (c) Subtraction image (b) − (a). The range is from −5.3 ppm (black) to 5.3 ppm (white). The average absolute error is 0.16 ppm. Note: There are regions where the experimental and the distorted SVC field map do not intersect (e.g., around the air cylinders) due to the peaks at air/tissue interfaces in the calculated map affecting the amount of distortion when Eq. (28) is applied. Therefore, (d) is included to eliminate these differences. (d) Subtraction image (b) − (a) in intersecting non-air regions. The range is from −1.31 (black) to 1.32 (white) ppm. Note: The lines on (b) indicate the placement of the scan lines in Fig. 8.

# P Majewski, A Materka: Approaches to MRI Simulation

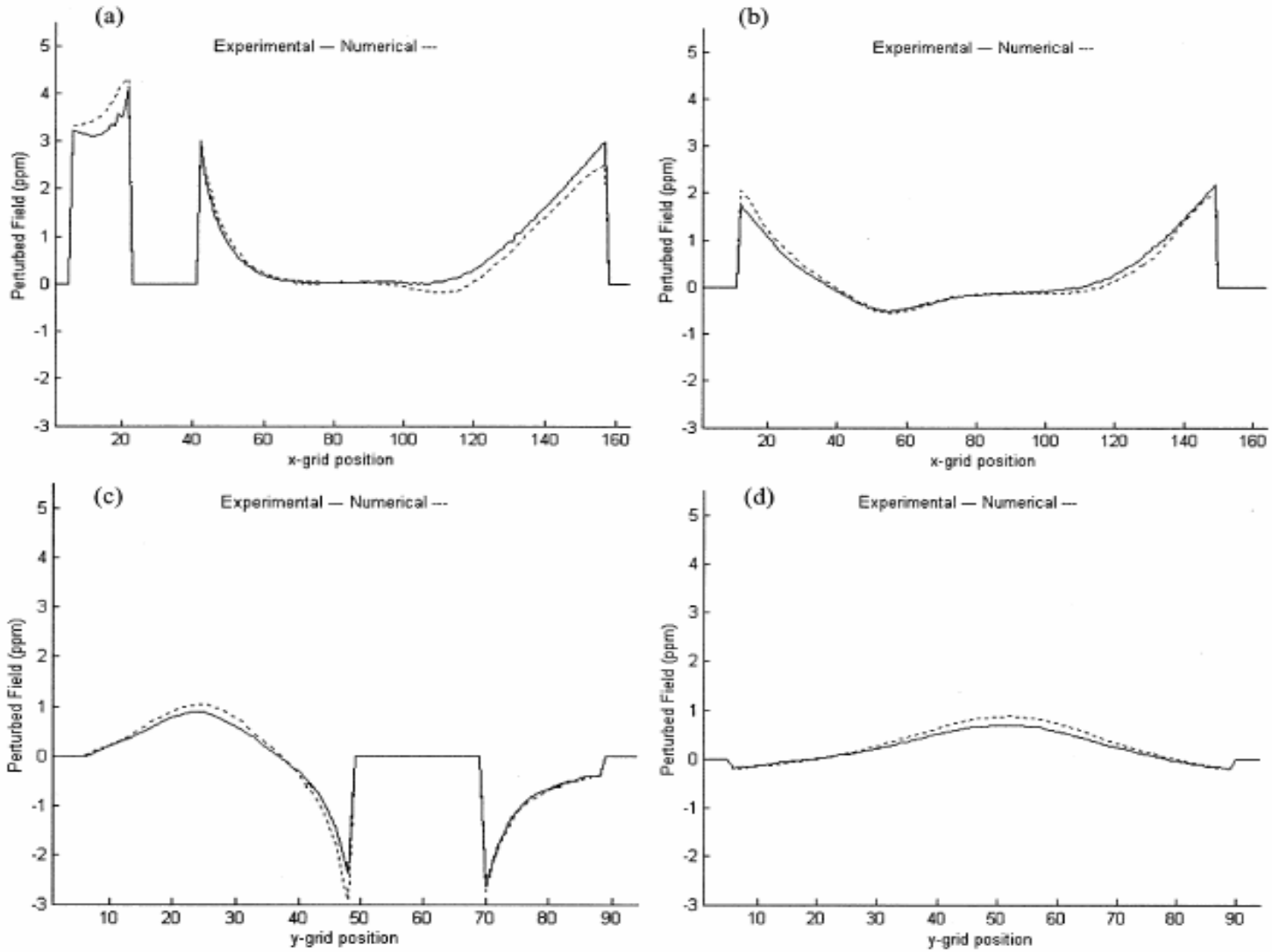


Fig. 8. The perturbation in the field along different scan lines of the sinus phantom. The experimental and SVC solutions are represented by solid and dashed lines, respectively. (a) Perturbed field along the black horizontal line in Fig. 7(b). The max absolute error is 0.7 ppm. (b) Perturbed field along the white horizontal line in Fig. 7(b). The max absolute error is 0.32 ppm. (c) Perturbed field along the black vertical line in Fig. 7(b). The max absolute error is 0.55 ppm. (d) Perturbed error along the white vertical line in Fig. 7(b). The max absolute error is 0.20 ppm.

## Validation (known analytic solution)

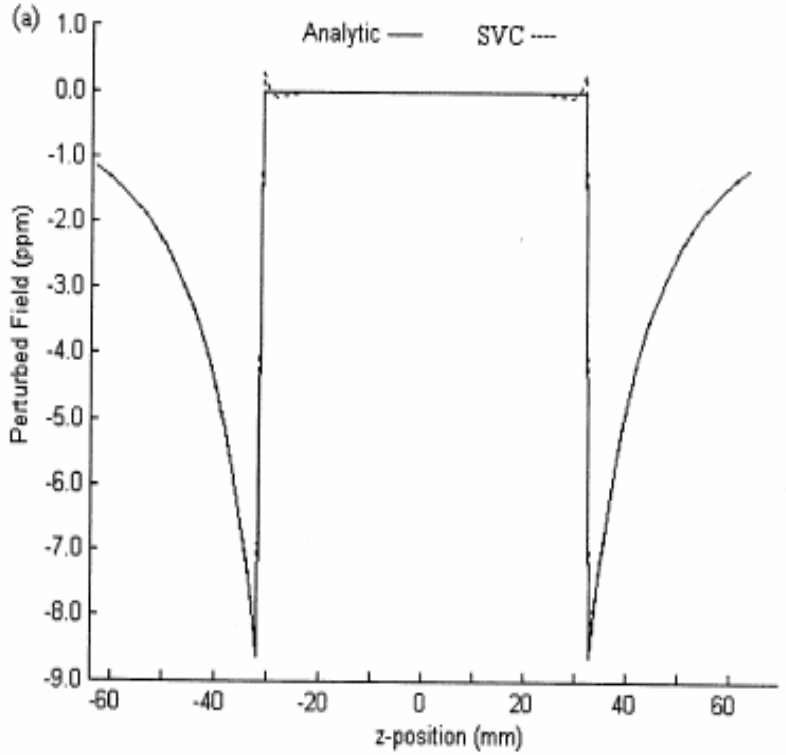


(a)

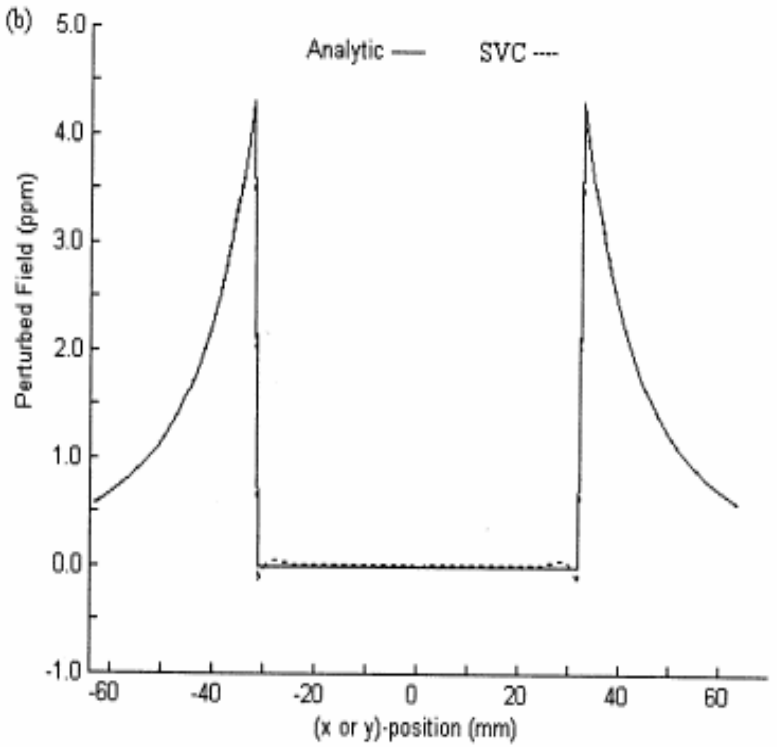


(b)

Fig. 1. The perturbation of the field along two orthogonal scan lines through the center of a sphere of water, $\chi = -9.05 \times 10^{-6}$, of radius 32 mm in a 1.5 T static field. Position 0 represents the center of the sphere. The analytic and SVC solutions are represented by solid and dashed lines, respectively. (a) The perturbed field along the $z$ axis. The maximum error is 0.3 ppm. (b) The perturbed field along the $x$ or $y$ axis. The maximum error is 0.15 ppm.

## *Part 2 – signal and image generation*

### *Object definition*

- every voxel's $T_1$, $T_2$, PD, frequency offset values

### *Event sequencer*

- RF pulse (start time, flip angle, duration of the pulse, axis about which to rotate)
- gradients ( start time, duration, amplitude)
- readout (start time, number of samples, sampling freqency, repetition time)

### *Simulator*

- executing the pulse sequence
- solving the Bloch equations to update each magnetization vector
- storing data (signal readout)

## Validation – part 2

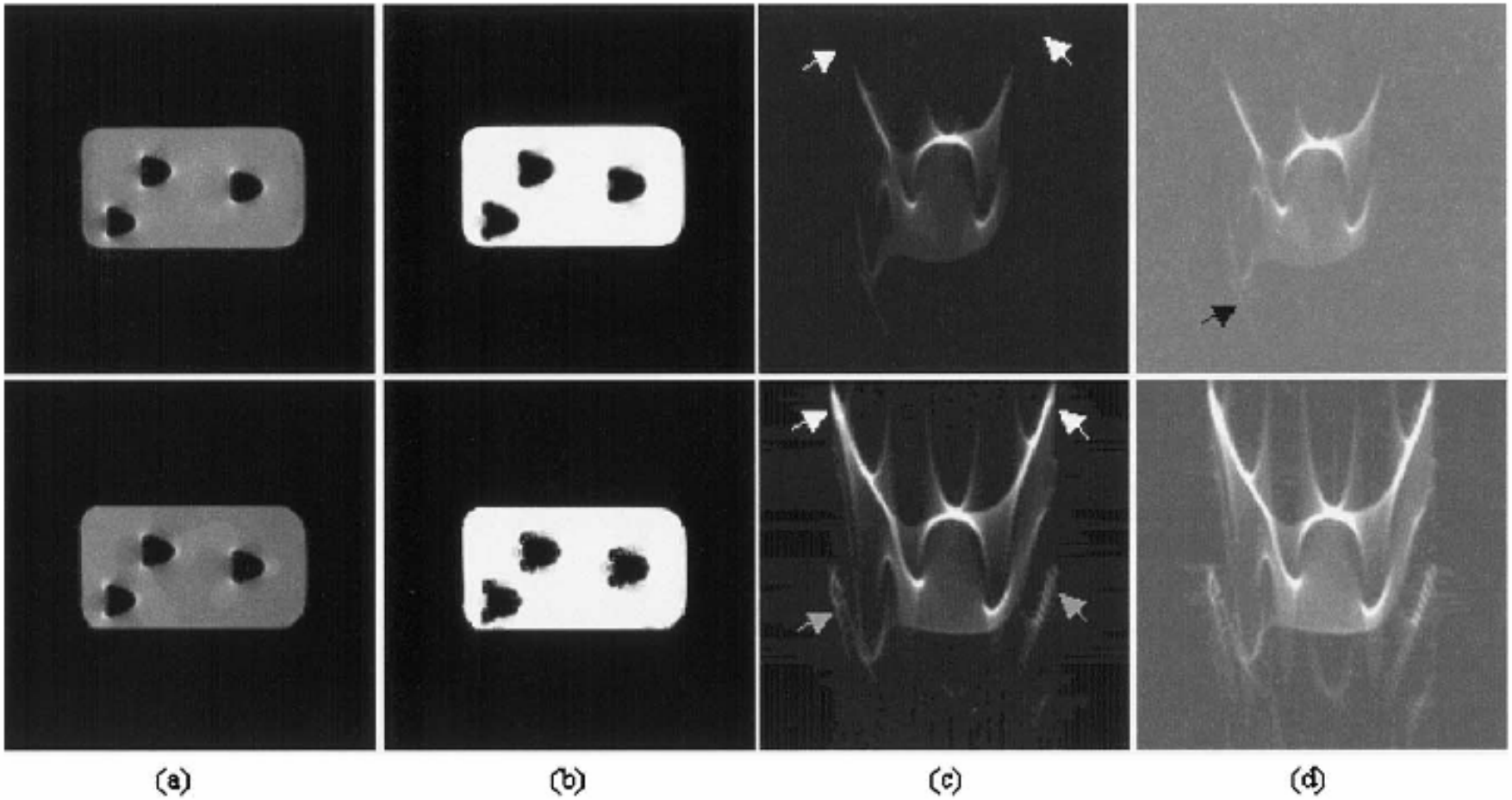


Fig. 10. Comparison of experimental (top row) and simulated (bottom row) images of sinus phantom. The frequency encoding direction is from left to right and the FOV = 20 cm for all images. The arrows highlight various features that are discussed in Section 3.2. (a) SE. Imaging parameters: TE = 20 ms, TR = 2000 ms, 256 × 256 imaging matrix. (b) GE. Imaging parameters: TE = 10 ms, TR = 800 ms, 256 × 256 imaging matrix. (c) SE EPI. Imaging parameters: TE = 180 ms, TR = 800 ms, 128 × 128 imaging matrix. (d) Same as (c) but with the window/level changed to reveal ghost artifacts.

## *Implementation - part 2*

- PC platform, MS Visual C ++ 6.0
- GUI dependent on Visual C++ objects, but the core can be compiled on other architectures
- computationally expensive

## *SIMRI – interactive 3D MRI simulator*

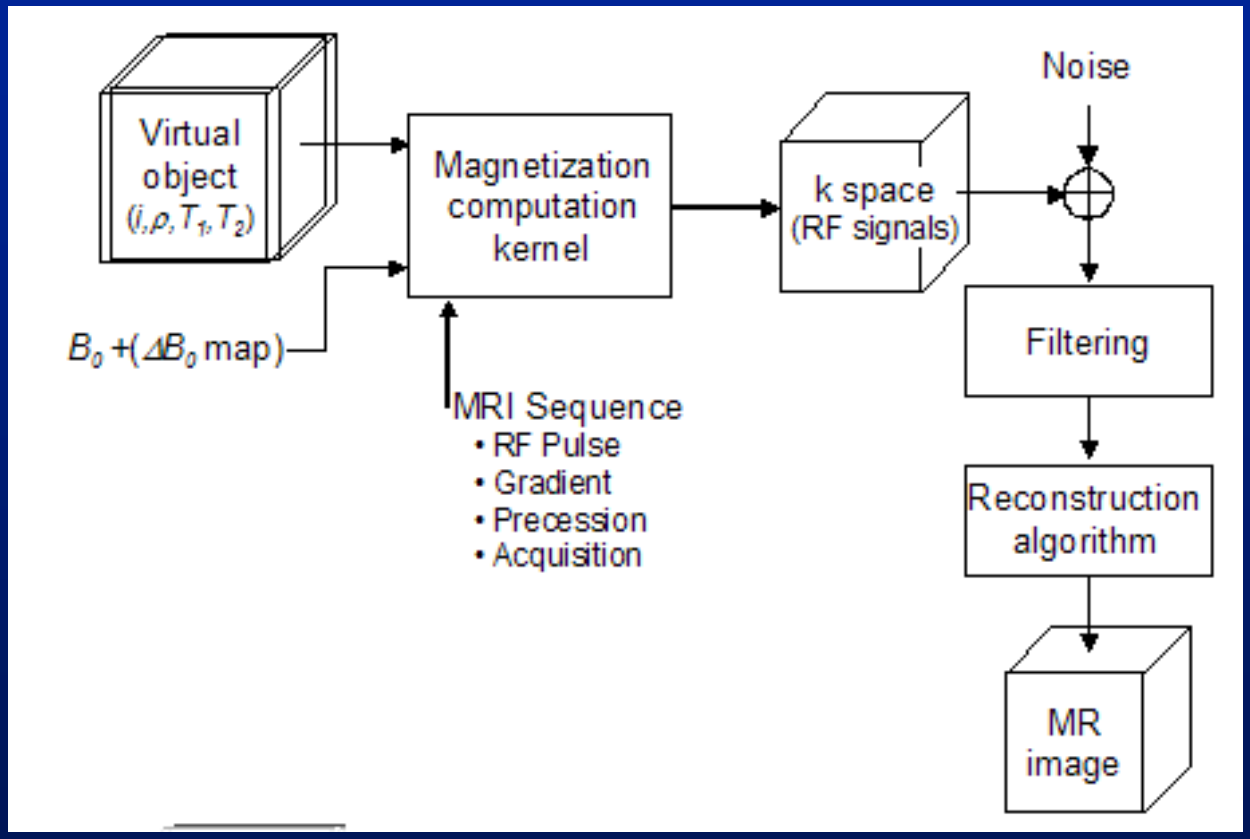


Benoit-Cattin H., Belaroussi B., Bellet F., Odet C, **2004, A versatile and interactive 3D MRI simulator, Journal of Magnetic Resonance**

## *SIMRI*

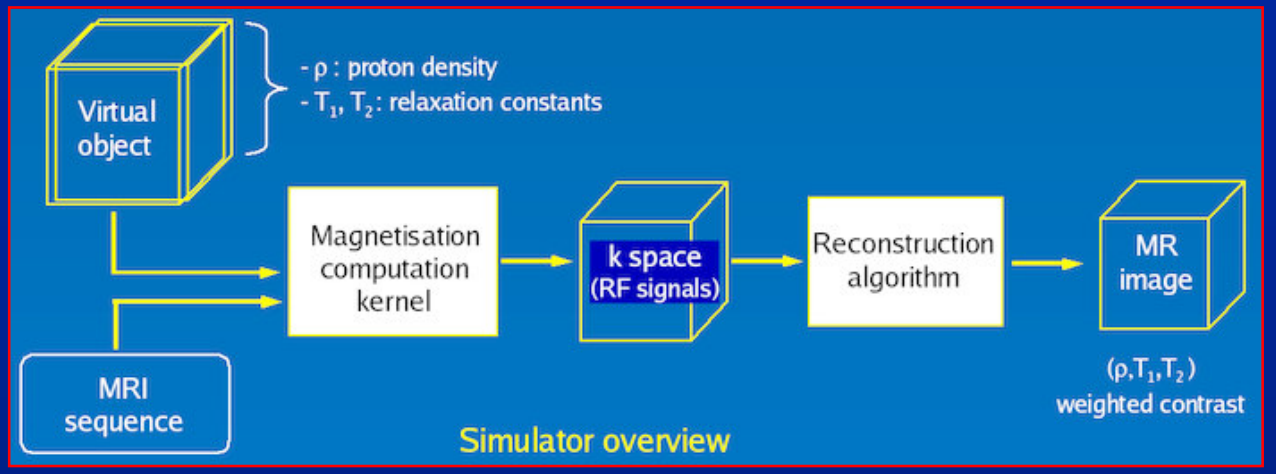


- based on Bloch equations
- T2* effect
- chemical shift artifact incl. off-resonance
- static field inhomogeneity
- susceptibility variation within an object

- spin echo
- gradient echo
- 1D, 2D, 3D images

- C programming language
- MRI programming: „high level" C functions with simple programming interface (Python)
- magnetization kernel: parrallel computing (PC grid architecture)
- 1D interactive interface to illustrate magnetization vector motion and MRI contrast

Benoit-Cattin H., Belaroussi B., Bellet F., Odet C, **2004, A versatile and interactive 3D MRI simulator, Journal of Magnetic Resonance**

## *„Montreal" phantom*

3-D high-resolution, anatomically accurate human brain phantom


Coronal, sagittal and transverse slices through CJH27, the (n=27) average MRI volume used to build the phantom.

### *Construction*

- preprocessing – intensity nonuniformity reduction
- automatic classification of preprocessed MRI volume
- manual correction of the classified data (% )

Collins D.L., et al., **1998, Design and Construction of a Realistic Digital Brain Phantom, IEEE Transactions on Medical Imaging**, 17:3

C.A. Cocosco C. A., et al., **1997, BrainWeb: Online Interface to a 3D MRI Simulated Brain Database, NeuroImage**, vol.5, no.4, part 2/4, S425.

# *„Montreal" phantom*

## *Phantom characteristics*

- high resolution (1 mm isotropic voxels) low-noise data set
- 27 scans (T1-w GE TR/TE/FA 18ms/10ms/$30^0$) of the same individual in stereotaxic space
- subsampled and intensity averaged
- the volume contains 181 x 217 x 181 voxels, covers the whole brain
- exhibits fine anatomical details normally obscured by noise in single image

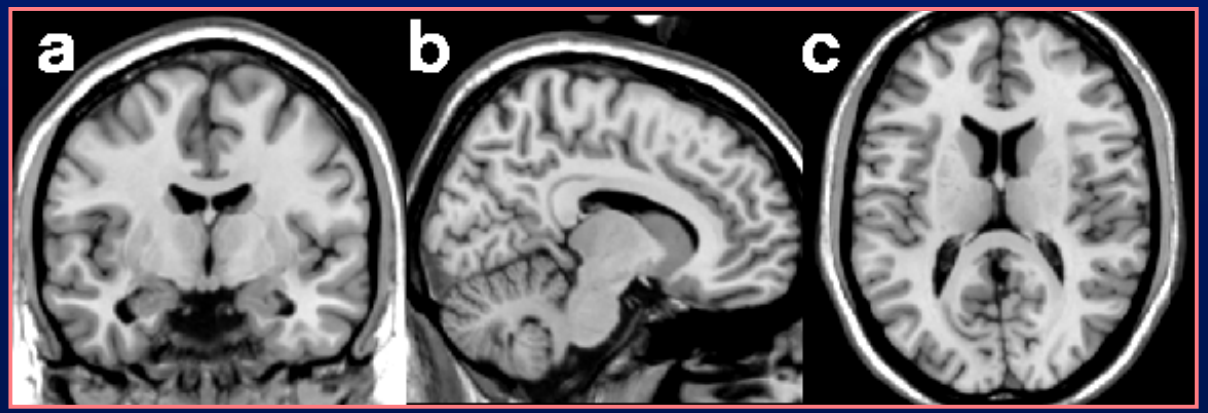

**Tissue volume definition**

| ID | Description |
|---|---|
| GM | grey matter within the brain parenchyma |
| WM | white matter within the brain parenchyma |
| CSF | cerebro spinal fluid surrounding the brain and within the ventricles |
| GL | layer of glial tissue lining the ventricles |
| M+S | muscle and skin |
| OTH | other tissue |
| FAT | fatty tissue |
| SKN | mostly skin |
| SKL | skull (does not include sinuses) |
| AIR | air outside head and within sinuses |

**BrainWeb:**
**Online Interface to a 3D MRI Simulated Brain Database**

CHRIS A. COCOSCO, VASKEN KOLLOKIAN, REMI K.-S. KWAN, G. BRUCE PIKE, ALAN C. EVANS

*McConnell Brain Imaging Centre, Montréal Neurological Institute,*
*McGill University, Montréal, Canada*

## *Application examples*

- study the performance of anatomical brain mapping techniques (relation to different MR acquisition parameters)
- validation of quantitative analyses for neuropathology (e.g. MS lesion quantification, medical pattern recognition and image processing techniques)

*http://www.bic.mni.mcgill.ca/brainweb/*

## *Custom MRI simulation*

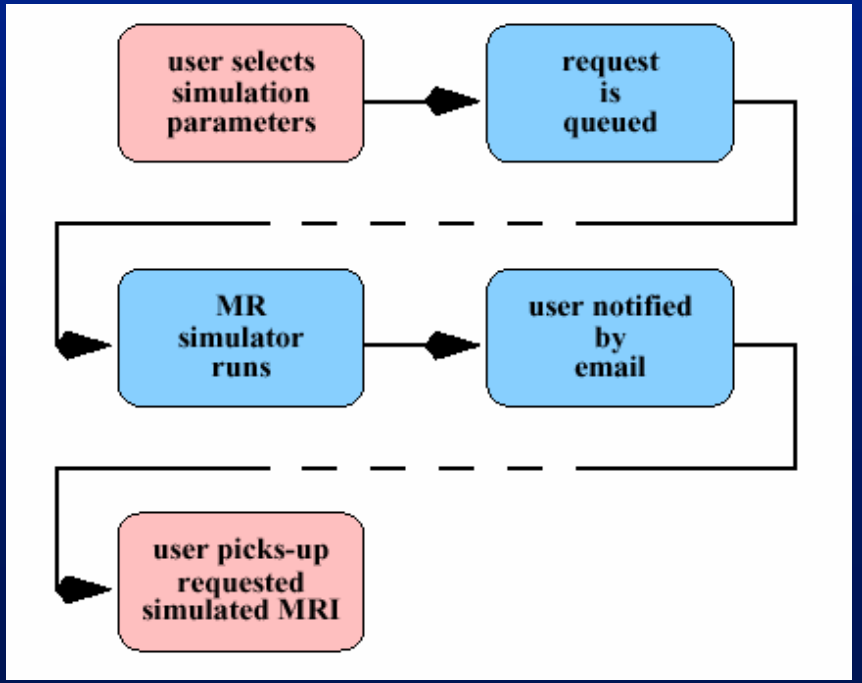

# On-line interface to Simulated Brain Database

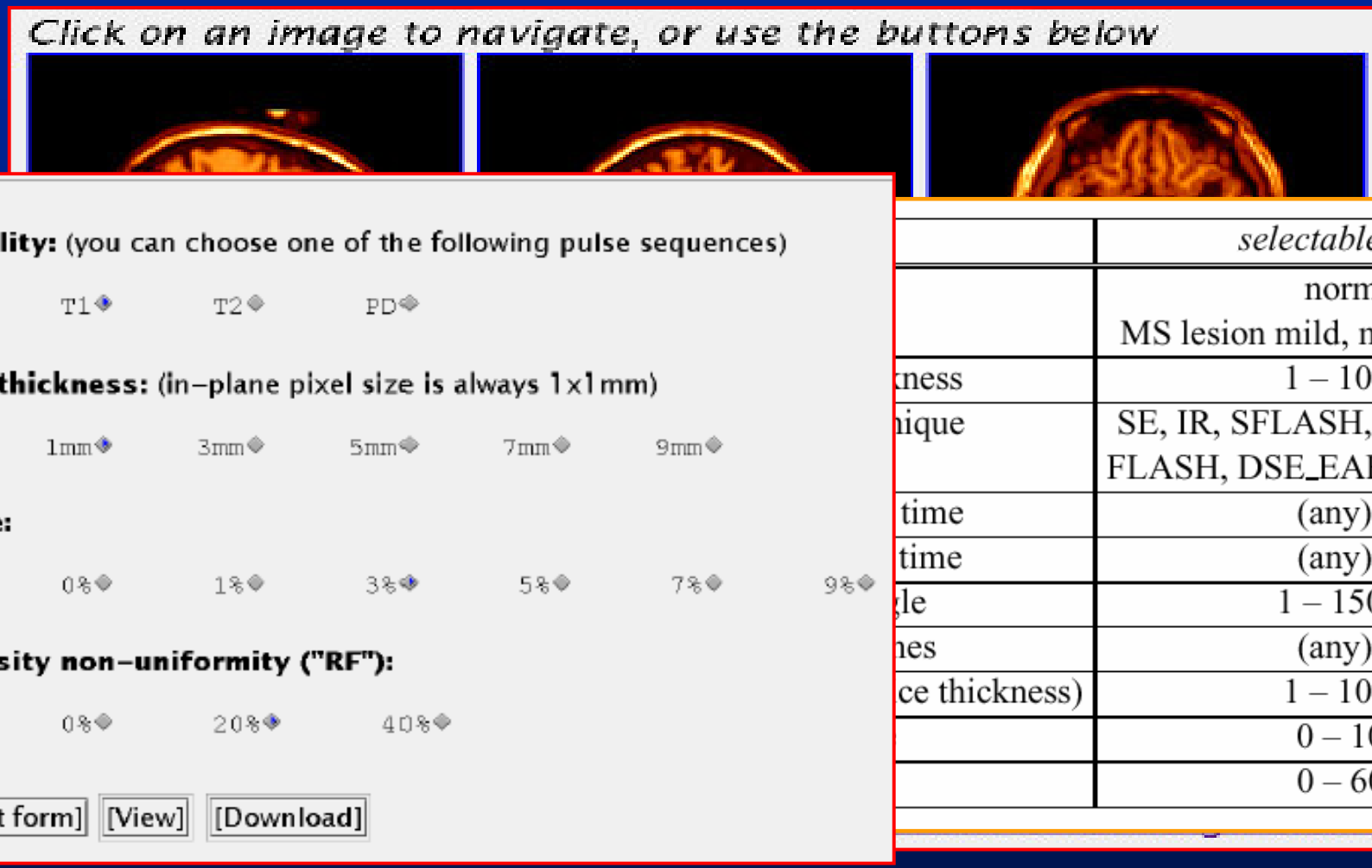


| | *selectable values* |
|---|---|
| | normal;<br>MS lesion mild, moderate, severe |
| ness | 1 – 10 mm |
| nique | SE, IR, SFLASH, CEFAST, FISP,<br>FLASH, DSE_EARLY, DSE_LATE |
| time | (any) ms |
| time | (any) ms |
| gle | 1 – 150 deg |
| nes | (any) ms |
| ce thickness) | 1 – 10 mm |
| | 0 – 10 % |
| | 0 – 60 % |

## *Questions*

- What kind of simulator is needed for COST B21?
- Can MRI ***texture*** be simulated?
- Can we share simulators?